Thermo-Optical "Canard Orbits" and Excitable Limit Cycles

Francesco Marino, Gustau Catalán, Pedro Sánchez, Salvador Balle, and Oreste Piro
Institut Mediterrani d'Estudis Avançats, CSIC–UIB, E-07071 Palma de Mallorca, Spain
(Received 25 July 2003; published 18 February 2004)

We demonstrate experimentally and theoretically the existence of canard orbits and excitable quasiharmonic limit cycles in the thermo-optical dynamics of semiconductor optical amplifiers. We also observe the phase locking of the noise-induced spikes to the small-amplitude Hopf quasiharmonic oscillations, recently predicted by Makarov, Nekorkin, and Velarde [Phys. Rev. Lett. **86**, 3431 (2001)].

DOI: 10.1103/PhysRevLett.92.073901 PACS numbers: 05.45.–a, 05.40.Ca, 42.65.Sf

Excitability and self-sustained relaxation oscillations are ubiquitous dynamical behaviors found in a wide range of systems including neural or cardiac cells and tissues, autocatalytic chemical reactions, electronic circuits, lasers and other optical systems, among many others [1,2]. Commonly, systems that exhibit excitable behavior in a range of parameters also have a regime of relaxation oscillations in another. Both regimes have been individually investigated in great extent under the most diverse experimental and theoretical conditions [3]. The transition from one type of behavior to the other lies within the known scenarios of the theory of bifurcations (Andronov saddle-node collisions, subcritical and supercritical Hopf bifurcations, etc.); however, the transitional regime exhibits special features associated with the almost singular character of the excitable dynamics, whose physical implications have only recently been investigated [4].

One of the most popular models to describe excitability and relaxation oscillations is the Van der Pol–FitzHugh-Nagumo (VdPFN) equation [5]

$$\dot{x} = y + x - x^3/3, \tag{1a}$$

$$\dot{y} = -\varepsilon(x - a) \tag{1b}$$

that describes a dynamical evolution with two very different characteristic time scales whose ratio is the small parameter ε. This model possesses a single steady state $x = a; y = a^3/3 - a$, which is stable for $|a| > 1$. In this regime the system displays excitable behavior for $|a|$ close to 1. A supercritical Hopf bifurcation occurs at the critical value $|a_c| = 1$ such that a quasiharmonic limit cycle develops with amplitude proportional to $\sqrt{a - a_c}$. However, the large split between time scales associated to the smallness of ε makes the quasiharmonic limit cycle observable only within a parameter range of order ε around the bifurcation point a_c. Outside this range the amplitude of the limit cycle abruptly (though continuously) jumps and reaches a saturation value, the so-called relaxation-oscillation regime. Likewise, the frequency of the oscillations experiences a similar sudden change from the quasiharmonic value — given by the imaginary part of the linear eigenvalues of the fixed point which is equal to $\varepsilon^{1/2}$ — to the relaxation-oscillation frequency proportional to ε. In the mathematical literature these sudden changes are known as "canard" explosions [6].

In the quasiharmonic regime, i.e., just above the Hopf bifurcation point, the system is still excitable: time-localized perturbations above a certain threshold induce large excursions in phase space, which are relatively insensitive to the details of the perturbation, before returning to the small globally attracting limit cycle. These excursions appear now as large pulses on a small-amplitude sinusoidal baseline. If the perturbations are in the form of sustained random noise, a succession of noise-triggered excitable pulses appears. Below the bifurcation point, these pulse trains have maximal regularity for an optimal nonzero value of the noise amplitude, a phenomenon known as coherence resonance [7,8]. Recently [1] it was beautifully demonstrated theoretically that just above the bifurcation these noise-induced excitable pulses appear synchronized to the quasiharmonic oscillation. This behavior, in turn, is reminiscent of the so-called stochastic resonance [9], where the pulses lock to an external periodic signal applied to the system. However, while sharing some features of both, the present effect should be considered as a third way between coherence and stochastic resonance, not the first because the interspike intervals are strongly correlated with the fixed quasiharmonic period, nor the second because there is no external forcing on the system. On the other hand, since the direct observation of canard phenomena is quite difficult due to the tiny range of parameters where they are bound to take place, this peculiar behavior under the action of noise — an unavoidable ingredient in real systems — constitutes a very useful experimental indicator for the presence of such regimes.

In this Letter we report what to our knowledge is the first experimental evidence of canard oscillations in an optical system. The system is a semiconductor optical amplifier (SOA) that may exhibit excitable and self-sustained thermo-optical pulsing regimes as either the injected power or the pumping current is increased. It has recently been shown that these regimes appear in an order compatible with the scenario of the VdPFN equations [10]. The experimental detection of the canard transition is then an amazing confirmation of the

correctness of such a dynamical scenario. We also show that a feasible physical model of the device contains all the observed behaviors (including canards) and can indeed provide the connection between the qualitative VdPFN description and the real physical variables.

In order to investigate the possible existence of the canard phenomenon, we first perform a careful experimental characterization of the transition from the excitable to the self-oscillatory regimes. To this effect, we use the same experimental setup described in [10], but here the SOA is a top-emitting vertical cavity surface emitting laser (VCSEL) biased below its threshold that operates in reflection mode. The VCSEL is an oxide-confined device, with an oxide window of 50 μm diameter and an optical cavity defined by two Bragg mirrors made of 17 n-type and 30 p-type pairs, respectively. The optical input (diameter $\sim$20 μm) is provided by a tunable external-cavity laser and enters the SOA cavity along the optical axis. The SOA output is monitored by an avalanche photodiode (1.6 GHZ bandwidth) connected to a digital oscilloscope (500 MHz bandwidth) (see [10] for details).

Figure 1 shows four traces of the output intensity as the pumping current is delicately increased within a properly chosen range. Trace (a) at the lowest value of this range corresponds to a steady state output in what we have previously called the excitable regime. Trace (d) at the other extreme of the range shows the so-called relaxation-oscillation regime. At transitional values of the pumping [trace (b)], the output starts performing very small-amplitude quasiharmonic oscillations due to a supercritical Hopf bifurcation. As expected from the VdPFN model, the quasiharmonic frequency is clearly higher than that of the relaxation-oscillation regime [see trace (d)]. However, for intermediate values of the current [trace (c)], the quasiharmonic output is sporadically interrupted by pulses quite similar in shape to those in the relaxation-oscillations regime. These pulses are, in fact, excitable responses randomly elicited by the small remanent noise unavoidable in the experiment. Further increasing the current above the value corresponding to trace (d) leads to a stable operation on the high power state through the reverse sequence but now with downward pulsing to the low-level output.

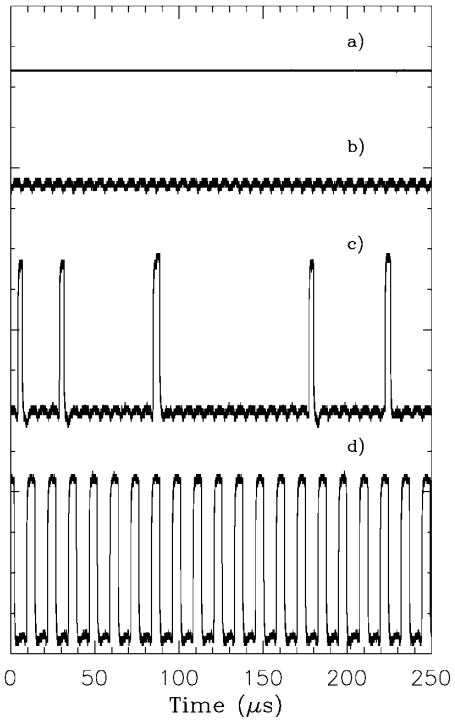

FIG. 1. Transition from excitable regime to self-oscillations in the amplifier output intensity as the pumping current is increased: (a) 179.9 mA, (b) 180.0 mA, (c) 180.1 mA, and (d) 180.2 mA. The vertical scale is 5 mV/div. An offset is artificially added to the series for the benefit of the display.

In the context of the VdPFN model, the statistical properties of noise-triggered excitable pulses have been studied mainly for the excitable regime just below the Hopf bifurcation in which the excitable state is the only fixed point of the system. In this case, the spikes are separated by an interval $T_p = T_r + T_a$, where T_r is the refractory time and T_a is the stochastic activation time which is continuously and unimodally distributed according to Kramers's law [11,12].

However, slightly above Hopf bifurcation where the excitable state is instead a quasiharmonic limit cycle, the statistical properties of the output change drastically. The distribution of interspikes times becomes multimodal because the probability of emitting a pulse is maximal at a specific phase of the quasiharmonic oscillation. This is revealed in Fig. 2 by the inter-spike-interval histogram exhibiting peaks centered at $t_n \approx T_r + n\tau$ $(n = 0, 1, 2, \ldots)$, being τ with the quasiharmonic period. In words, the train of noise-triggered excitable pulses is stochastically synchronized to the small-amplitude limit cycle [1]. This behavior could be considered similar to the stochastic resonance observed when an excitable system is driven by both an external periodic signal and noise [13,14]. In our case, however, there is no external modulation: it is the small cycle, intrinsic to the autonomous dynamics, that is responsible for the features described above. In addition, since the period of the quasiharmonic cycle is shorter than the refractory time, the first peak of the histogram does not correspond to the quasiharmonic oscillation period but to the refractory time instead. Finally, by increasing the noise level [Fig. 2(b)] the firing efficiency of the noise increases and the amplitude of the first peak of the histogram increases relatively to the others.

In Fig. 3 we have plotted a phase-space projection reconstructed from a low-pass filtered experimental time series by means of a minimal application of the Ruelle-Takens embedding technique using only one time delay. This reconstruction shows all the essential features that one expects in the noisy version of the canards regime as it has been reported in a previous

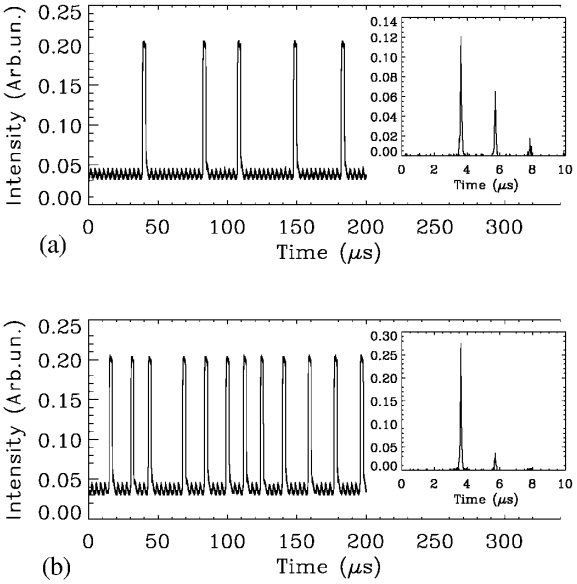

FIG. 2. Time traces and corresponding interpulse time histogram in the quasiharmonic regime, in the presence of external noise (50 MHz bandwidth) generated by an Agilent 33250A arbitrary waveform generator. The noise is added to the pumping current by means of a bias tee, and the rms. noise levels are 0.25 mA (upper trace) and 0.5 mA (lower trace).

theoretical analysis of FitzHugh-Nagumo–like models [1]. This fact corroborates the suitability of the VdPFN scenario for the description of the thermo-optical dynamics of SOAs that was proposed in [10].

The physics of thermal effects has been theoretically investigated in a number of optical systems such as parametric oscillators [15] and semiconductor etalons [16,17]. In these cases, the coupling of temperature to the faster optical and material variables often leads to a self-oscillatory behavior instead of the expected optical bistability due to the interaction of the carrier density with the optical field [18]. This breakdown of bistability is due to the fact that the same interaction makes the temperature vary, thus inducing a refractive index change that shifts the cavity resonance thereby modifying the intracavity field. A physical model for our particular system can be constructed from the standard traveling-wave description of a SOA,

$$\partial_t E_\pm \pm v\partial_z E_\pm = \frac{v}{2}\Gamma a(N - N_t)(1 - i\alpha)E_\pm, \quad (2)$$

$$\partial_t N = J - \gamma_{\rm sp} N - v a(N - N_t)(|E_+|^2 + |E_+|^2), \quad (3)$$

where $E_\pm$ are the slowly varying amplitudes of the forward and backward fields around the optical carrier frequency Ω, v is the group velocity, Γ is the optical confinement factor, a is the differential material gain, N is the carrier density, N_t is the transparency carrier density, α is the linewidth enhancement factor, J is the number of carriers per unit time and unit volume injected into the active region, and $\gamma_{\rm sp}$ is the nonstimulated carrier recombination rate. The boundary conditions for the above equations read $E_+(0,t) = r_1 E_-(0,t) + t_1' E_i$, $E_-(L,t) = r_2 e^{i2\Omega n/cL} E_+(L,t)$, where n is the effective index in the SOA waveguide, L is the length of the SOA, $r_{1,2}(t_{1,2})$ are the amplitude reflection (transmission) coefficients of the front and rear facets as seen from the inside of the SOA, while the prime denotes the same quantities as seen from the outside, and E_i is the injected field. The reflected and transmitted fields are thus given by $E_r = r_1' E_i + t_1 E_-(0,t)$, $E_t = t_2 e^{i\Omega n/cL} E_+(L,t)$. We consider that the effective index n depends linearly on temperature T, which evolves according to

$$\partial_t T = -\gamma_{\rm th}(T - T_s - R_{\rm th} H), \quad (4)$$

where $\gamma_{\rm th}$ is the relaxation rate of T towards its equilibrium value, T_s is the substrate temperature fixed by the Peltier element, $R_{\rm th}$ is the thermal impedance of the device, and H is the power dissipated in the device. From an energy balance [19] it is found that $H = VI + A(|E_i|^2 - |E_r|^2 - |E_t|^2) - B\gamma_{\rm sp} N$, where V is the voltage applied to the SOA, I is the total current injected into the SOA, and A (B) is the power extracted by a photon emitted by stimulated (spontaneous) emission.

Assuming that the fields follow adiabatically the evolution of the (much slower) other variables and upon suitable rescaling [20], the model can be recast in the form

$$\dot{G} = \gamma_{\rm sp}(G_0 - G - P_i Q), \quad (5a)$$

$$\dot{\phi} = -\gamma_{\rm th}(\phi - \phi_e + \lambda G + \mu P_i Q), \quad (5b)$$

$$Q = \frac{(1 - R_1)(1 + R_2 e^G)(e^G - 1)}{1 + R_1 R_2 e^{2G} - 2\sqrt{R_1 R_2} e^G \cos(\phi - \alpha G)}, \quad (5c)$$

where G is the single-pass gain in the amplifier, G_0 is the unsaturated single-pass gain arising from current injection, P_i is the optical input power, ϕ is the normalized detuning between the input field and the cavity resonance, ϕ_e is its equilibrium value without optical emission, λG

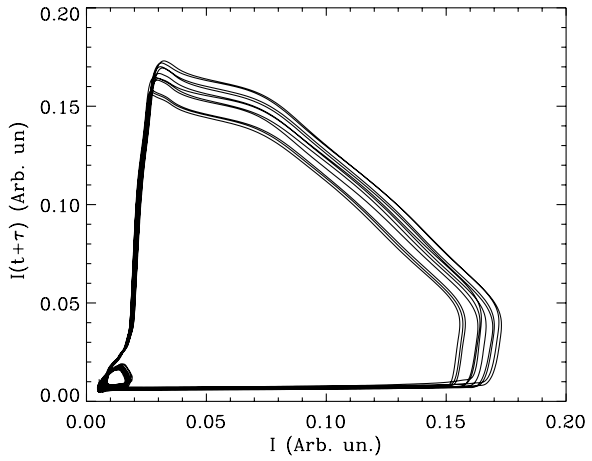

FIG. 3. Experimental reconstruction of the phase space through one time-delay Ruelle-Takens embedding technique: The time delay is 0.6 μs.

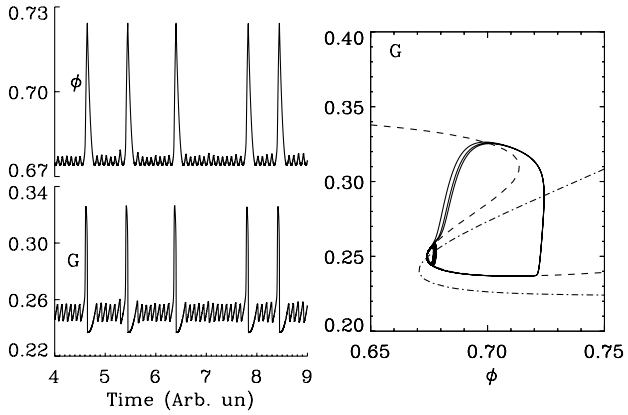

FIG. 4. Time series of ϕ and G and the corresponding phase-space trajectory, obtained by numerical integration of Eqs. (5) in the presence of additive Gaussian white noise. The parameters values are $G_0 = 0.357$, $\phi_e = 0.8899$, $P_i = 0.005$, $\mu = 2$, $R_1 = 0.49$, $R_2 = 0.999$, $\lambda = 0.005$, $\alpha = 3$, and $\gamma_{sp}/\gamma_{th} = 0.015$. The noise intensity is $D = 10^{-3}$.

is the correction to ϕ due to spontaneous emission, and $\mu P_i Q$ is that due to stimulated emission. Current noise is included as a white, random Gaussian variation of G_0.

Equations (5) are equivalent to the spatially homogeneous case in [16] by considering a negative absorption (i.e., gain) and adding the pumping term G_0. The difference is that in our case we do not consider any thermal dependence of the parameters, but only the variations in cavity detuning due to the optothermal coupling. In Fig. 4 we plot the phase portrait of the system (dotted line) together with the nullclines of Eqs. (5) (solid lines) for parameters in the canard region. The nullcline corresponding to $\dot{G} = 0$(dashed line) is a Z-shaped manifold arising from the Airy function in Q, while that corresponding to $\dot{\phi} = 0$ (dot-dashed line) has the shape of a "i" whose upper branch is an almost straight line. The structure of the nullclines is therefore analogous to that in the generic VdPFN model, which supports the hypothesis made in [10] of an underlying VdPFN scenario for the thermo-optical pulsations observed in SOAs. Moreover, the trajectories in phase space clearly display the canard structure, corresponding in this case to the emission of noise-triggered excitable pulses which are stochastically synchronized to a small-amplitude quasiharmonic limit cycle, as can be seen in the time traces for G and ϕ shown in the lower panel of Fig. 4.

In summary, we have experimentally demonstrated the existence of canard orbits and excitable quasiharmonic limit cycles in the thermo-optical dynamics of semiconductor optical amplifier. We have also observed the stochastic synchronization of the noise-induced spikes with the small-amplitude Hopf quasiharmonic oscillations leading to a multipeaked interspike intervals distribution with peaks separated by the period of the quasiharmonic oscillation. This canard phenomenon can have interesting applications in signal processing (e.g., optical clock regeneration or detection of low-level signals) since it was shown [4] that the addition of a signal at the quasiharmonic frequency may amplify stochastic resonance in these systems. Moreover, this phenomenon provides a way for regularizing the spiking of the system in a noisy environment without requiring an external forcing of the system [1]. We have finally shown that a physical model for the system possesses a phase-space structure equivalent to that in the simpler VdPFN model.

We acknowledge financial support from MCYT and MEC (Spain) through Project No. TIC2002-04255, Project CONOCE (BFM2000-1108), and Sabbatical Grant No. PR2002-0329.

[1] V. A. Makarov, V. I. Nekorkin, and M. G. Velarde, Phys. Rev. Lett. **86**, 3431 (2001)
[2] V. I. Krinsky, in *Self Organization, Autowaves and Structures far from Equilibrium*, edited by V. I. Krinsky (Springer, Berlin, 1984), pp. 9–19; A. M. Zhabotinskii, *Concentration Autooscillations* (Nauka, Moscow, 1974); T. Frisch, S. Rica, P. Coullet, and J. M. Gilli, Phys. Rev. Lett. **72**, 1471 (1994); P. Coullet, D. Daboussy, and J. R. Tredicce, Phys. Rev. E **58**, 5347 (1998); M. Giudici, C. Green, G. Giacomelli, U. Nespolo, and J. R. Tredicce, Phys. Rev. E **55**, 6414 (1997).
[3] J. D. Murray, *Mathematical Biology* (Springer-Verlag, Berlin, 1989).
[4] E. I. Volkov, E. Ullner, A. A. Zaikin, and J. Kurths, Phys. Rev. E, **68**, 026214 (2003).
[5] R. FitzHugh, Biophys. J. **1**, 445 (1961); J. Nagumo, S. Arimoto, and S. Yoshizawa, Proc. IREE Aust. **50**, 2061 (1962).
[6] J. L. Callot, F. Diener, and M. Diener, C. R. Acad. Sci. Ser. 1 **286**, 1059 (1978).
[7] A. Pikovsky and J. Kurths, Phys. Rev. Lett. **78**, 775 (1997).
[8] G. Giacomelli, M. Giudici, S. Balle, and J. R. Tredicce, Phys. Rev. Lett. **84**, 3298 (2000).
[9] L. Gammaitoni, P. Hanggi, P. Jung, and F. Marchesoni, Rev. Mod. Phys. **70**, 223 (1998).
[10] S. Barland, O. Piro, S. Balle, M. Giudici, and J. Tredicce, Phys. Rev. E **68**, 036209 (2003).
[11] H. Kramers, Physica (Utrecht) **7**, 284 (1940).
[12] M. C. Eguia, G. B. Mindlin, and M. Giudici, Phys. Rev. E **58**, 2636 (1998).
[13] K. Wiesenfeld *et al.*, Phys. Rev. Lett. **72**, 2125 (1994).
[14] F. Marino, M. Giudici, S. Barland, and S. Balle, Phys. Rev. Lett. **88**, 040601 (2002).
[15] P. Suret *et al.*, Phys. Rev. A **61**, 021805(R) (2000).
[16] Yu. A. Rzhanov, H. Richardson, A. A. Hagberg, and J.V. Moloney, Phys. Rev. A**47**, 1480 (1993).
[17] E. Abraham, Opt. Commun. **61**, 282 (1987).
[18] H. Kawaguchi, *Bistabilities and Nonlinearities in Laser Diodes* (Artech House, Boston, 1994).
[19] B. Mroziewicz, M. Bugajski, and W. Nakwaski, *Physics of Semiconductor Lasers* (North-Holland, Amsterdam, 1991).
[20] Details of the derivation will be published elsewhere.